

Assembly of the inner rod determines needle length in the type III secretion injectisome

Thomas C. Marlovits^{1,2†}, Tomoko Kubori^{1†}, María Lara-Tejero¹, Dennis Thomas³, Vinzenz M. Unger² & Jorge E. Galán¹

Assembly of multi-component supramolecular machines is fundamental to biology, yet in most cases, assembly pathways and their control are poorly understood. An example is the type III secretion machine, which mediates the transfer of bacterial virulence proteins into host cells¹. A central component of this nanomachine is the needle complex or injectisome, an organelle associated with the bacterial envelope that is composed of a multi-ring base, an inner rod, and a protruding needle². Assembly of this organelle proceeds in sequential steps that require the reprogramming of the secretion machine. Here we provide evidence that, in *Salmonella typhimurium*, completion of the assembly of the inner rod determines the size of the needle substructure. Assembly of the inner rod, which is regulated by the InvJ protein, triggers conformational changes on the cytoplasmic side of the injectisome, reprogramming the secretion apparatus to stop secretion of the needle protein.

Type III secretion systems (TTSSs) are present in many bacteria pathogenic for humans, animals or plants^{1,3}. An essential component of this system is the 'needle complex' or 'injectisome', which is composed of a multi-ring base and a protruding needle (Supplementary Fig. S1a). In *Salmonella* spp., the cause of food poisoning and typhoid fever, the base is composed of three proteins, namely InvG, PrgH and PrgK (ref. 4). The needle, which is composed of a single protein, PrgI, is connected to a different substructure, the inner rod, which traverses the entire length of the base and is made of PrgJ (ref. 5). The inner rod is anchored to a socket-like structure on the basal side of the base, which may serve as an adaptor between the helical inner rod and the N-fold symmetric base⁵. The entire needle complex is traversed by a channel that serves as a conduit for the passage of proteins that travel the type III secretion pathway. Assembly of the needle complex involves the formation of the base, which upon recruitment of several accessory proteins, proceeds to secrete exclusively the proteins that make up the needle and inner rod substructures⁶. Once the needle reaches a certain length, the TTSS switches substrate specificity and becomes competent for the secretion of effector proteins that are to be delivered into the host cell. In *Salmonella*, the length of the needle and the substrate switching of the secretion machine depends on the accessory protein InvJ (refs 4, 7). Consequently, strains lacking InvJ assemble injectisomes with much longer needles and cannot secrete effector proteins. The mechanisms by which InvJ carries out its function are poorly understood. A *Yersinia* spp. homologue of InvJ, YscP, has been proposed to work as a 'molecular ruler'. YscP would function as an extended polypeptide anchored to the tip of the growing needle and the base of the needle complex⁸. Its full extension would signal that

the needle has reached the appropriate length, conveying information to the secretion apparatus to switch substrates.

To investigate the mechanism of needle-length control and substrate switching in TTSSs, we compared by electron cryomicroscopy the detailed structural organization of needle complexes obtained from wild-type and $\Delta invJ$ *S. typhimurium* mutant strains. As previously observed⁴, needle complexes obtained from the $\Delta invJ$ *S. typhimurium* strain exhibited very long needle filaments (Supplementary Fig. S1b). In sharp contrast with wild-type needle complexes, however, the needles of these injectisomes became easily detached upon isolation and were almost never seen attached to the base (Supplementary Fig. S1b). As previously reported for wild type⁵, the base of the injectisomes of the $\Delta invJ$ mutant strain exhibit heterogeneous symmetries ranging from 19- to 22-fold, with 20- and 21-fold corresponding to the most abundant species (data not shown). Images from complexes isolated from $\Delta invJ$ *S. typhimurium* were sorted in different symmetry classes, and the three-dimensional structure for the 20-fold needle complex was reconstructed at 20 Å resolution (Supplementary Figs S2 and S3). Overall, the surface rendering of the needle complex of $\Delta invJ$ *S. typhimurium* shows no significant difference with that of wild type, exhibiting similar disposition and appearance of the outer and inner rings and their subunits⁵ (Fig. 1).

The cropping of the reconstruction of the $\Delta invJ$ *S. typhimurium* needle complex, however, revealed very significant structural differences within the base. Most notably, all particles isolated from the

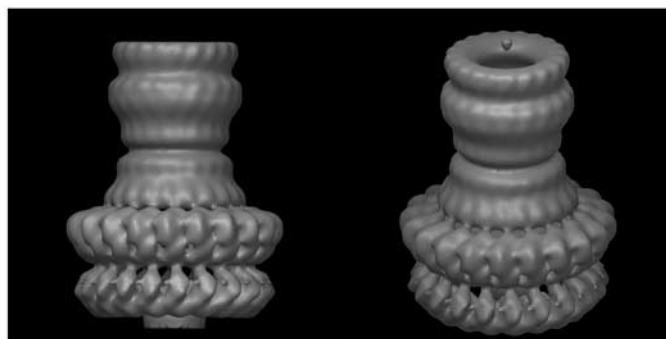


Figure 1 | Structure of TTSS injectisome obtained from $\Delta invJ$ *S. typhimurium*. Surface rendering of the structure of the $\Delta invJ$ *S. typhimurium* needle complex. Shown here is the structure of the 20-fold complex with 20-fold symmetry imposed (left panel, lateral view; right panel, tilted view).

¹Section of Microbial Pathogenesis, Yale University School of Medicine, Boyer Center for Molecular Medicine, New Haven, Connecticut 06536, USA. ²Department of Molecular Biophysics and Biochemistry, Yale University School of Medicine, New Haven, Connecticut 06520-8024, USA. ³Howard Hughes Medical Institute, Rosenstiel Basic Medical Sciences Research Center, Department of Biochemistry, Brandeis University, Waltham, Massachusetts 02454, USA. [†]Present addresses: Research Institute of Molecular Pathology (IMP) and Institute of Molecular Biotechnology, Austrian Academy of Sciences (IMBA), Dr Bohr-Gasse 5, A-1030 Vienna, Austria (T.C.M.); 21st Century COE Program, Combined Program on Microbiology and Immunology, Osaka University, 3-1 Yamadaoka, Suita, Osaka 565-0871, Japan (T.K.).

$\Delta invJ$ mutant lacked the inner rod substructure that traverses the base (Fig. 2a). Consistent with this observation, PrgJ, the main component of the inner rod⁵, was not detected in needle complexes obtained from the $\Delta invJ$ mutant strain (Fig. 2b) although this protein was readily detected in culture supernatants free from the shed needles^{4,9}. In addition, most of the $\Delta invJ$ particles lacked the characteristic 'socket' present on the basal plate of the base chamber of the wild-type injectisomes (Fig. 2a). The difference between the density maps of bases obtained from wild type and the $\Delta invJ$ mutant (Fig. 2c) indicates that the changes are indeed largely localized to the socket structure, so 'misalignments' between the two structures cannot account for the observed differences. As InvJ is not an integral component of the base^{2,4}, we hypothesize that this protein may help to stabilize the appropriate conformation of the socket that allows the 'docking' of PrgJ and the initiation (or termination) of the assembly of the inner rod. The failure of PrgJ to assemble into inner rods in the absence of InvJ, and its presence in culture supernatants of the $\Delta invJ$ mutant⁹, are consistent with this hypothesis.

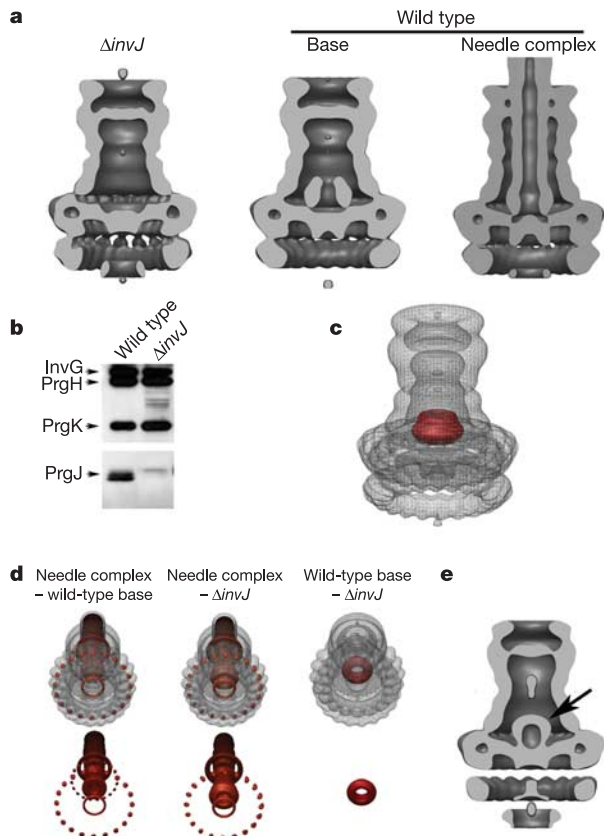


Figure 2 | Structural differences between needle complexes of wild-type, $\Delta invJ$ and $\Delta prgJ$ *S. typhimurium*. **a**, Cropping of the surface renderings of the $\Delta invJ$ injectisome base reveals the absence of the socket-like structure and the inner rod observed in the wild-type base and needle complexes, respectively. **b**, PrgJ, the main component of the inner rod, is absent from *S. typhimurium* $\Delta invJ$ needle complexes. Needle complexes obtained from wild-type and $\Delta invJ$ *S. typhimurium* strains were analysed by western immunoblotting. **c**, The difference between the density maps (indicated in red) of the wild-type (mesh) and the $\Delta invJ$ mutant base structures indicates that the socket is absent from the $\Delta invJ$ base. **d**, The density maps of the wild-type or $\Delta invJ$ base were subtracted from the maps of the fully assembled needle complex or the wild-type base, as indicated. The differences between the density maps are indicated in red, and the densities of the subtracted structures are indicated by mesh. The different structures are shown tilted forward 60°. **e**, Cropping of the surface rendering of the structure of the $\Delta prgJ$ injectisome base revealing the presence of the socket-like structure (arrow) that is observed in the wild-type base.

We have previously shown that the transition from the base to the fully assembled needle complex results in very significant conformational changes in the base substructure³. In addition to significant conformational changes observed within the base to accommodate the inner rod and needle, marked conformational changes were observed on the cytoplasmic face of the base substructure, which we hypothesized may provide the structural bases for substrate switching upon needle assembly⁵. Notably, a cup-like protrusion located on the cytoplasmic face of the base substructure, which may serve as entry point for proteins that travel this pathway, undergoes a significant 'downward' movement, therefore appearing longer in the fully assembled needle complex. Furthermore, completion of the needle complex results in significant conformational changes in one of the inner rings of the base, further redefining the shape of its cytoplasmic face³. The tilted views of the difference between the density maps of bases obtained from wild type and the $\Delta invJ$ mutant revealed that the cup-like protrusion on the cytoplasmic face is significantly shorter than that of the wild-type fully-assembled needle complexes (Fig. 2d). Additional conformational changes were also detected in one of the inner rings (Fig. 2d). Indeed, the cytoplasmic face of the $\Delta invJ$ base closely resembles that of the base substructure of the wild-type injectisome before needle assembly (Fig. 2d). This observation is consistent with the phenotype of the $\Delta invJ$ mutant, which is unable to undergo substrate switching and is therefore 'locked' in a secretion mode similar to that of the base before needle assembly—that is, competent for the secretion of the needle and inner rod proteins PrgI and PrgJ, but unable to secrete effector proteins^{4,6,7}.

We determined the three-dimensional structure of needle complexes obtained from a *S. typhimurium* $\Delta prgJ$ mutant. Although the resolution of this structure is lower than those of the $\Delta invJ$ and wild type (Supplementary Fig. S1), the cropping of this reconstruction

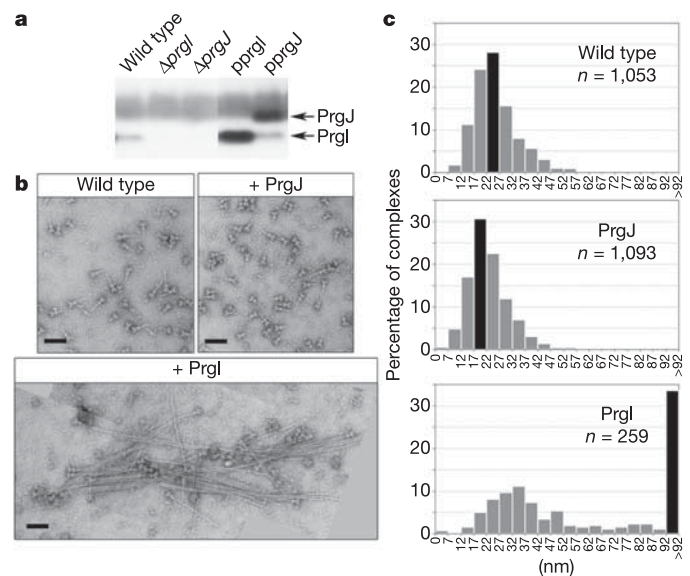


Figure 3 | Altering the stoichiometry between the needle and rod proteins results in injectisome needles of different lengths. **a**, Western immunoblot analysis of needle complexes from strains overexpressing the needle protein PrgI (labelled pprgI) or the inner rod protein PrgJ (labelled pprgJ). **b**, Electron micrographs of negatively stained needle complexes from *S. typhimurium* strains overexpressing either PrgI or PrgJ, as indicated. Scale bars, 100 nm. **c**, Measurements of needle length in needle complexes from wild-type *S. typhimurium* and derivative strains overexpressing either PrgI or PrgJ, as indicated. Dark bars denote the most abundant size of the measured species and *n* denotes the number of particles measured. The differences between the needle size of wild-type and PrgJ or PrgI overexpressing strains were statistically significant ($P < 0.0001$).

(Fig. 2e) clearly revealed the presence of the socket within the base, arguing that the stabilization of the socket and presumably the subsequent assembly of the inner rod is not the result of the direct interaction between InvJ with PrgJ. Rather, these results indirectly argue in favour of the hypothesis that InvJ exerts its function on the components of the base (that is, PrgH/PrgK) either directly or indirectly through interactions with other accessory proteins.

The observation that the $\Delta invJ$ mutant, which lacks the inner rod, produces needles indicates that needle assembly *per se* does not require the inner rod. However, the resulting needles in the $\Delta invJ$ mutant are loosely linked to the base and easily detach during purification (Supplementary Fig. S1b), indicating that assembly of the inner rod may be required for the proper anchoring of the needle substructure. Without the inner rod the type III secretion organelle is unable to secrete effector proteins and remains locked in a conformation that is only competent for the secretion of PrgI and PrgJ (refs 4, 6, 7). Therefore, termination of the assembly of the inner rod may be necessary to induce conformational changes that may be required for substrate switching, thereby controlling needle length. If this were the case, the needle length should be influenced by the relative concentration of the inner rod and needle proteins PrgJ and PrgI, which in turn may influence the speed at which each of the substructures is assembled.

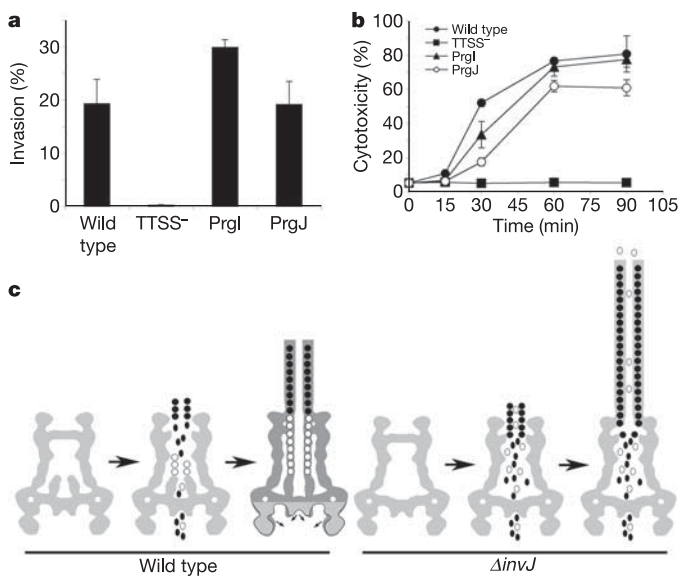


Figure 4 | Altering needle length by changes in the stoichiometry of the needle and inner rod proteins results in functional injectisomes. a, Levels of internalization into cultured epithelial cells of wild-type and TTSS-defective (TTSS⁻) *S. typhimurium* and derivative strains overexpressing either the needle protein PrgI or the inner rod protein PrgJ. Values are the means \pm standard deviation of three independent measurements, and represent the percentage of the inoculum that survived treatment with gentamicin, an indication of bacterial internalization. **b**, Macrophage cytotoxicity of wild-type and TTSS-defective *S. typhimurium* and strain derivatives overexpressing either PrgI or PrgJ. Cytotoxicity was determined by assaying LDH release. Values represent the means \pm standard deviation of three independent measurements and were standardized to 100% release obtained by complete cell lysis. **c**, Model of needle length control. Assembly of the inner rod but not the needle requires InvJ. Completion of the inner rod leads to conformational changes on the cytoplasmic side of the injectisome, which results in substrate switching and the interruption of secretion of the inner rod and needle proteins, hence determining the length of the needle substructure. In the absence of InvJ, the socket of the base is not formed and the inner rod fails to assemble. Consequently, the secretion machinery remains locked in a secretion mode competent for the secretion of the needle protein, resulting in non-functional injectisomes with abnormally long needles. Filled circles, needle protein PrgI; open circles, inner rod protein PrgJ.

To test this hypothesis, we constructed *S. typhimurium* strains that overexpress either PrgI or PrgJ (Fig. 3a) and examined the length of the needles in isolated needle complexes. Overexpression of PrgI resulted in injectisomes with needles significantly ($P < 0.0001$) longer than wild type (Fig. 3b). In fact, a significant proportion of the needles were too long to be accurately measured as they could not be observed in a single field of view. Unlike the long needles observed in the $\Delta invJ$ mutant strain (Fig. 1b), however, the vast majority of the long needles in the PrgI overexpressing strain were firmly attached to the base (Fig. 3b and c). Injectisomes obtained from a strain overexpressing PrgJ had needles that were significantly ($P < 0.0001$) shorter than wild type (Fig. 3b and c). Other than the different length of the needles, injectisomes obtained from these strains appeared identical to wild type. These results indicate that altering the stoichiometry of the inner rod and needle proteins has a profound impact on the length of the needle substructure.

To ascertain whether needle complexes with needles of different length assembled by *S. typhimurium* strains with an altered PrgI/PrgJ stoichiometry were functional, we examined two phenotypes that are known to depend on this TTSS: bacterial internalization into epithelial cells and cytotoxicity towards macrophages¹⁰. *S. typhimurium* overexpressing PrgI, which leads to longer needles, entered epithelial cells with slightly higher efficiency than wild type, although its cytotoxicity towards macrophages was not altered (Fig. 4a and b). This is in sharp contrast with the $\Delta invJ$ mutant, which exhibits longer needles but has a non-functional TTSS and is unable to enter epithelial cells^{7,11}. A strain overexpressing PrgJ, which leads to shorter needles, showed a slight decrease in macrophage cytotoxicity although it was not altered in its ability to enter epithelial cells (Fig. 4a and b). These results indicate that needles of different length caused by changes in the stoichiometry of PrgI and PrgJ are indeed functional.

Taken together, our results suggest a model for the mechanisms of needle-length control (Fig. 4c). Completion of the inner rod would result in the firm anchoring of the needle to the base, triggering conformational changes on the cytoplasmic side of the injectisome and reprogramming of the secretion apparatus to stop secretion of the needle and inner rod proteins. In this model, InvJ is required to stabilize a conformation of the socket of the injectisome base that is permissive for the anchoring of the inner rod. In the absence of InvJ, the socket is not formed, the inner rod fails to assemble or anchor, and the secretion machinery remains locked in a secretion mode that is competent for the secretion of the needle protein but not the effectors, resulting in non-functional injectisomes with abnormally long needles. The function of InvJ would be similar to that proposed for scaffolding proteins involved in flagellar assembly, which, like InvJ, do not form part of the final flagellar structure and are secreted to the culture medium^{12,13}. InvJ may therefore function as a 'kinetic trap', allowing the socket to go from a flexible, unstructured state to a state competent for interactions with the inner rod protein PrgI. Consistent with this hypothesis, conformational heterogeneity in the 'socket' region of the needle complex can be detected when lowering the threshold of the reconstruction of the $\Delta invJ$ structure. Although TTSSs are largely conserved, more experiments will be required to extend the generality of this proposed mechanism to related systems in other bacteria.

METHODS

Bacterial strains and plasmids. All *Sallmonella enterica* serovar Typhimurium (*S. typhimurium*) were derived from strain SJW2941 and have been previously described⁶. Plasmids expressing either the PrgI or PrgJ protein were constructed by standard recombinant DNA techniques using the plasmid expression vector pWSK29 (ref. 14).

Bacterial invasion and macrophage cytotoxicity assays. The ability of the different *S. typhimurium* strains to invade cultured intestinal epithelial cells or to kill cultured J774 macrophages was assayed by the gentamicin resistance and LDH (lactic dehydrogenase) release assays, respectively, as previously described^{15,16}.

Needle complex preparation and analysis, electron microscopy, and image processing. Needle complex sample preparation for electron microscopy, biochemical analysis, electron microscopy, image processing and the determination of the rotational symmetry was carried out as previously described⁵ with some modifications (see Supplementary Methods).

Determination of needle length in needle complexes. Needle complex preparations from the different bacterial strains grown to late stationary phase were prepared as described elsewhere⁵. To avoid size bias during isolation, all caesium chloride fractions were pooled before measurement. Samples were placed on glow-discharged Cu/Rh grids and negatively stained using 2% PTA (phospho-tungstic acid pH 7.2). Electron microscopic images were recorded with a 1K CCD camera using a Technai T12 electron microscope equipped with a LaB6-filament operated at 120 kV and 30,000× magnification. Each pixel corresponded to a sampling of 5.5 Å at the level of the specimen. To determine the length of individual needle filaments protruding from the base, three data points were recorded: (1) the centre of inner ring 1, (2) the centre of outer ring 1, and (3) the tip of the needle filament (see Supplementary Fig. S1a). To account for tilted particles in the recordings, the length of the filaments (that is, the distance between (2) and (3)) was normalized to the constant distance between IR1 and OR1 (distance between (1) and (2)). Statistical analysis was carried out using the Mann–Whitney test.

Received 3 April; accepted 19 April 2006.

- Galán, J. E. & Collmer, A. Type III secretion machines: bacterial devices for protein delivery into host cells. *Science* **284**, 1322–1328 (1999).
- Kubori, T. *et al.* Supramolecular structure of the *Salmonella typhimurium* type III protein secretion system. *Science* **280**, 602–605 (1998).
- Cornelis, G. R. & Van Gijsegem, F. Assembly and function of type III secretory systems. *Annu. Rev. Microbiol.* **54**, 735–774 (2000).
- Kubori, T., Sukhan, A., Aizawa, S. I. & Galán, J. E. Molecular characterization and assembly of the needle complex of the *Salmonella typhimurium* type III protein secretion system. *Proc. Natl Acad. Sci. USA* **97**, 10225–10230 (2000).
- Marlovits, T. C. *et al.* Structural insights into the assembly of the type III secretion needle complex. *Science* **306**, 1040–1042 (2004).
- Sukhan, A., Kubori, T., Wilson, J. & Galán, J. E. Genetic analysis of assembly of the *Salmonella enterica* serovar Typhimurium type III secretion-associated needle complex. *J. Bacteriol.* **183**, 1159–1167 (2001).
- Collazo, C. & Galán, J. E. Requirement of exported proteins for secretion through the invasion-associated Type III system in *Salmonella typhimurium*. *Infect. Immun.* **64**, 3524–3531 (1996).
- Journet, L., Agrain, C., Broz, P. & Cornelis, G. R. The needle length of bacterial injectisomes is determined by a molecular ruler. *Science* **302**, 1757–1760 (2003).
- Sukhan, A., Kubori, T. & Galán, J. E. Synthesis and localization of the *Salmonella* SPI-1 type III secretion needle complex proteins PrgI and PrgJ. *J. Bacteriol.* **185**, 3480–3483 (2003).
- Galán, J. E. *Salmonella* interaction with host cells: Type III secretion at work. *Annu. Rev. Cell Dev. Biol.* **17**, 53–86 (2001).
- Collazo, C. M., Zierler, M. K. & Galán, J. E. Functional analysis of the *Salmonella typhimurium* invasion genes *invI* and *invJ* and identification of a target of the protein secretion apparatus encoded in the *inv* locus. *Mol. Microbiol.* **15**, 25–38 (1995).
- Macnab, R. How bacteria assemble flagella. *Annu. Rev. Microbiol.* **57**, 77–100 (2003).
- Macnab, R. Type III flagellar protein export and flagellar assembly. *Biochim. Biophys. Acta* **1694**, 207–217 (2004).
- Wang, R. F. & Kushner, S. R. Construction of versatile low-copy-number vectors for cloning, sequencing and gene expression in *Escherichia coli*. *Gene* **100**, 195–199 (1991).
- Chen, L. M., Kaniga, K. & Galán, J. E. *Salmonella* spp. are cytotoxic for cultured macrophages. *Mol. Microbiol.* **21**, 1101–1115 (1996).
- Galán, J. E. & Curtiss, R. III Cloning and molecular characterization of genes whose products allow *Salmonella typhimurium* to penetrate tissue culture cells. *Proc. Natl Acad. Sci. USA* **86**, 6383–6387 (1989).

Supplementary Information is linked to the online version of the paper at www.nature.com/nature.

Acknowledgements We thank members of the Galán laboratory for critical reviews of this manuscript. We are also grateful to the Yale School of Medicine for the support of the Cryo Electron Microscopy Core Facility. Molecular graphic images were produced using the Chimera package from the Computer Graphics Laboratory, University of California, San Francisco (supported by the NIH). This work was supported by grants from the National Institutes of Health (to V.M.U. and J.E.G.).

Author Information The three-dimensional density maps have been deposited into the EBI-MSD EMD database under the accession code EMD-1214. Reprints and permissions information is available at npg.nature.com/reprintsandpermissions. The authors declare no competing financial interests. Correspondence and requests for materials should be addressed to J.E.G. (jorge.galan@yale.edu).